

Redox-switchable Intramolecular π - π -Stacking of Perylene Bisimide Dyes in a Cyclophane

Felix Schlosser, Michael Moos, Christoph Lambert,* and Frank Würthner*

Dedicated to Professor Waldemar Adam on the occasion of his 75th birthday

Inspired by increasingly detailed insights into nature's highly sophisticated machinery for the transformation of chemical, redox or light energy into mechanical motion, there is a strong impetus on chemists to develop similarly masterful nanodevices.^[1-9] Towards this goal there is a need for (supra)molecular functional units whose size, shape and arrangements in space can be controlled by external stimuli such as light, electrons or ions. In a most general sense, such supramolecular functional nanodevices may be called artificial molecular machines.^[1] Depending on additional design features, such units might be further developed towards molecular motors.^[2] Originating from several decades of pioneering basic research,^[3] the currently most widely investigated and already quite sophisticated artificial molecular machines are given by catenanes and rotaxanes,^[4] for which rotational or translational motion could be directed by photo- or electrochemical triggers and even solid state switching devices with hysteretic (bistable) current/voltage characteristics could be demonstrated.^[5,6] Other ingenious molecular machines include sterically congested alkenes, whose sequential photo- and thermal isomerization processes afforded unidirectional rotations which could be applied to spin nanoparticles and macroscopic objects.^[7] Furthermore, pronounced conformational changes have been reported for a number of azobenzene-based photoswitches upon irradiation with light,^[8] and for calixarene-tethered oligothiophenes upon oxidation.^[9]

Based on the rather limited number of molecular and supramolecular scaffolds applied in this field of research, there is a clear incentive to look for new building blocks whose conformation and functional properties can be controlled by external stimuli. In our opinion aggregates of functional dyes^[10] are such candidates, in particular if they are composed of building blocks such as perylene bisimides (PBI) which are known to exhibit pronounced stability in their neutral form as well as for various oxidized and reduced states.^[11] Although a myriad of self-assembled and covalently tethered PBI aggregates have been reported during the last decade,^[12] to the best of our knowledge, there is no report that elucidates conformational changes of the PBI

aggregate structure upon electrochemical oxidation or reduction.^[13] Thus, based on prior molecular modeling studies, we have designed and synthesized PBI cyclophane **8** (Scheme 1) and elucidated its response on stepwise electrochemical reduction, which provided unambiguous proof for a pronounced conformational transition from a *closed* cavity with co-facially stacked PBIs in the neutral state to an expanded *open* cavity of the three- and fourfold reduced state. While redox active cyclophanes have been investigated extensively,^[14,15] such a structural transformation upon charging appears to be novel in this context.

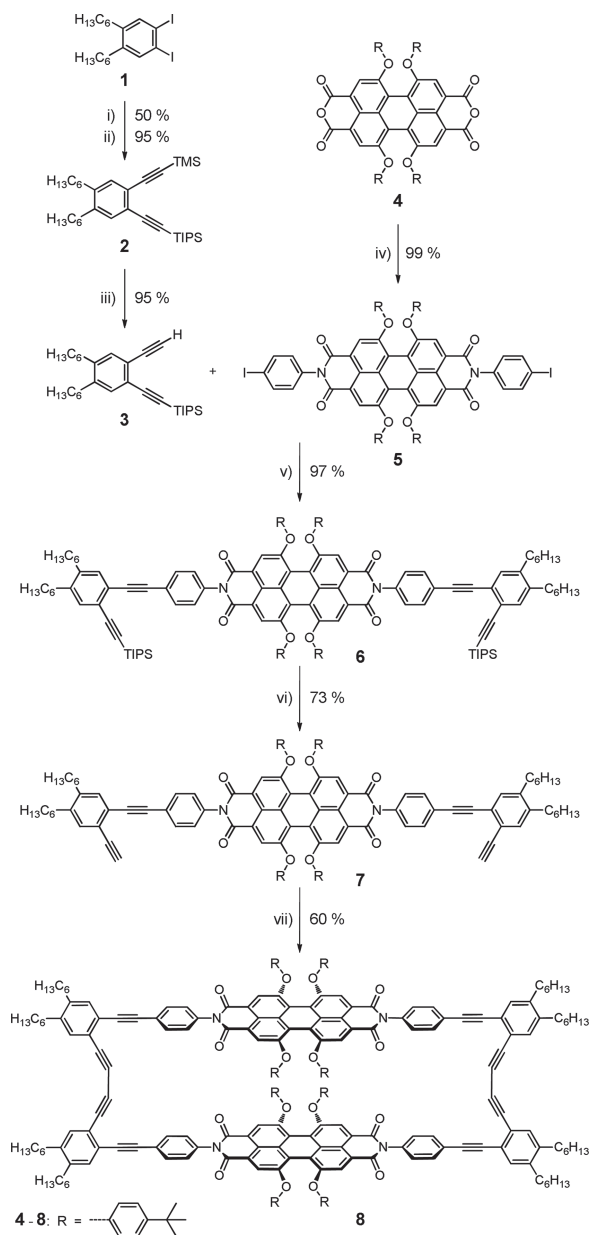
The synthesis of PBI cyclophane **8** is shown in Scheme 1. It is based on the one-step cyclo-oligomerization that, according to common understanding,^[16] has to be carried out under high dilution to favor the second intramolecular cyclization step over intermolecular oligomer formation. After initial studies with different coupling methods (i.e. oxidative Glaser and Hay couplings) we opted for the more promising Pd/Cu-catalyzed Sonogashira coupling conditions^[17] that here, in the absence of a haloarene, led to the oxidative diacetylene homocoupling product **8** in a remarkably high yield of 60%. Notably, this high yield could be obtained under rather "normal" conditions, i.e. with 40 mg precursor PBI **7** dissolved in 60 mL THF under argon atmosphere at 60 °C. To rationalize this excellent yield of cyclized product, we may assume that the precursor molecules are already templated^[18] in a bimolecular PBI-PBI-complex^[19] or that at least the intermediate mono-coupled product exhibits ideally preorganized acetylenic units for the subsequent macrocyclization. All preceding reaction steps (Scheme 1) from 4,5-dihexyl-1,2-diiodobenzene^[20] and 1,6,7,12-tetra(4-*tert*-butylphenoxy)perylene bisanhydride **4** were rather straightforward with mostly high yields.

The structural properties of PBI **8** were investigated by NMR, UV-vis and fluorescence spectroscopy, which all supported the assumed dye arrangement based on molecular modeling (Figure 1). Thus, in the UV-vis absorption spectra (Figure 1a), a pronounced excitonic coupling of the two PBI dyes is evident by the reversal of the band intensities at around 540 and 580 nm. This reversal in intensity is highly indicative for PBI dyes that are helically stacked at close distance (Figure 1b) and originates from a complex interplay of excitonic and vibronic couplings (so-called intermediate coupling regime).^[21,22] Notably, this kind of cofacial PBI-PBI stacking arrangement has not been observed before for self-assembled PBIs equipped with four phenoxy substituents in bay positions,^[19] but is the energetically favored PBI-PBI arrangement for the parent PBIs that bear hydrogen atoms at bay positions.^[13] No spectral broadening is observed for the PBI-related absorption bands from 400–650 nm for PBI

F. Schlosser, M. Moos, Prof. C. Lambert,
Prof. F. Würthner
Universität Würzburg
Institut für Organische Chemie & Center for
Nanosystems Chemistry
Am Hubland, 97074 Würzburg, Germany
E-mail: christoph.lambert@uni-wuerzburg.de;
wuerthner@chemie.uni-wuerzburg.de



DOI: 10.1002/adma.201201266



Scheme 1. Synthesis of perylene bisimide cyclophane **8**. Reagents and conditions: i) trimethylsilylacetylene, Pd(PPh₃)₂Cl₂, CuI, HNⁱPr₂, rt, 15 h; ii) triisopropylsilylacetylene, Pd(PPh₃)₂Cl₂, CuI, HNⁱPr₂, rt, 20 h; iii) THF, MeOH, KOH, H₂O, rt, 1 h; iv) 4-iodoaniline, imidazole, 120 °C, 5 h; v) Pd(PPh₃)₂Cl₂, CuI, HNⁱPr₂, THF, 60 °C, 20 h; vi) *n*Bu₄NF, THF, rt, 4 h; vii) Pd(PPh₃)₂Cl₂, CuI, HNⁱPr₂, THF, 60 °C, 22 h.

8 in comparison with PBI **5**, which is consistent with a rather rigid supramolecular architecture. Likewise the sharp features of the diphenyldiacetylene absorption band at <400 nm complies with rigidity. The fluorescence spectrum of PBI **8** shows a large Stokes shift, a lack of vibronic structure and a decrease in fluorescence quantum yield from 100% (PBI **5**) to 6% (PBI **8**). In compliance with our earlier work on self-assembled PBI π -stacks these features may be attributed to a change in the mutual arrangement of the two PBI chromophores in the excited state.^[13]

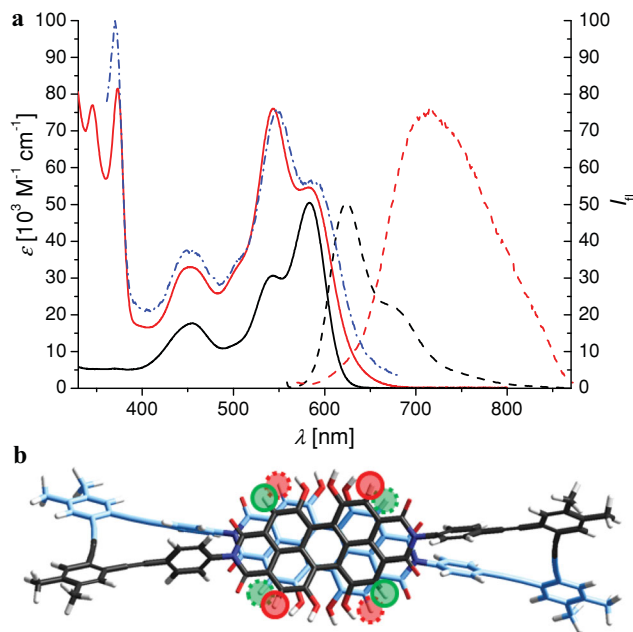


Figure 1. a) UV-vis absorption (solid lines) and fluorescence spectra (dashed lines, $\lambda_{\text{ex}} = 545 \text{ nm}$) of PBI **8** (red) and PBI **5** (black), and fluorescence excitation spectrum of PBI **8** (blue, dashed-dotted line, $\lambda_{\text{det}} = 700 \text{ nm}$) in dichloromethane at room temperature. b) Structural model according to MM+ calculations with assignment of magnetically non-equivalent PBI protons (marked in red and green); for better clarity, the lower lying carbons are of light blue color and the bulky *tert*-butylphenoxy groups are replaced by hydrogen. Notably, only the arrangement with *P*-helicity is depicted although the molecules consist of a 1:1 mixture of *P*- and *M*-helical PBI stacks.

Even more direct evidence for the structural model comes from NMR spectroscopy. Accordingly, the characteristic ¹H singlet signals of PBI core protons 2, 5, 8 and 11 (marked red and green in Figure 1b) are split into two singlet signals, and the AA'BB' spin systems of aromatic protons of the *tert*-butylphenoxy subunits are split into two sets of signals (see Supporting Information, Figure S1), which is in agreement with a D₂-symmetric chiral scaffold as depicted in Figure 1b. To examine the flexibility of the PBI macrocycle **8** temperature-dependent ¹H NMR measurements were performed (see Supporting Information, Figure S2). At higher temperatures coalescence into a single signal is observed for the signals of perylene protons 2, 5, 8 and 11, as well as for the aromatic proton signals of *tert*-butylphenoxy subunits. These changes suggest a higher symmetry species and may be attributed to a flipping process between the *P*- and *M*-helical PBI-PBI arrangements that is now faster than the NMR timescale (for structural model, see Figure S3 in Supporting Information). In the transition state the PBI chromophores are expected to arrange in a parallel orientation with respect to their N-N-axis concomitant with a loss of chirality and an increase of distance between the PBI π -faces.

The dynamic of the flipping process of PBI **8** was investigated further by calculating the free activation enthalpy ΔG^\ddagger using Equation (1) according to the coalescence method^[23]

$$\Delta G^\ddagger = R \cdot T_c \cdot \ln \left(\frac{R \cdot T_c \cdot \sqrt{2}}{\pi \cdot N_A \cdot h \cdot \Delta \nu} \right) \quad (1)$$

where R , N_A and h are the gas constant, the Avogadro constant and the Planck constant, respectively, T_c is the coalescence temperature and $\Delta \nu$ is the frequency difference between the interconverting protons observed in the low temperature regime. The perylene core protons, as well as the *tert*-butylphenoxy protons, are well suited for this purpose because of the simple determination of their coalescence temperatures from line broadening. Coalescence temperatures for perylene and *tert*-butylphenoxy protons of 344 K and 333 K, respectively, have been determined. The frequency differences of the respective proton signals at low temperature are 131.3 Hz and 62.3 Hz. With these values, a free activation enthalpy ΔG^\ddagger of 68 kJ mol⁻¹ was calculated in each case (see Table S1 in Supporting Information) which corresponds to a rate constant of 138 s⁻¹ for the oscillating movement of the PBIs between the two *M*- and *P*-helical conformations at a temperature of 333 K.^[23]

While proton NMR measurements thus give evidence for a thermally activated structural rearrangement (interconversion of *P*- and *M*-helical cyclophane **8**), reduction of the PBI moieties in **8** induces another molecular motion in the PBI cyclophane, a widening of the macrocyclic ring with a concomitant separation of the PBI π -faces. Cyclic voltammetry (CV) of **8** in dichloromethane shows dynamic behavior with increasing scan rate (0.250–10 V s⁻¹, see Figure 2a and also Figure S4 in Supporting Information) which can be digitally simulated using DigiSim^[24] by assuming an EEECE mechanism. This mechanism involves stepwise reduction of the cyclophane (PBI^{••}PBI → PBI^{•••}PBI → PBI^{••••}PBI) to the dianion in which both PBIs are singly charged (see Figure 3). These two processes are well resolved in the CV at -0.964 V and -1.148 V vs Fc/Fc⁺ (values given are those from the digital fit with an estimated accuracy of ± 5 mV. The analogous first redox potential of the reference compound **7** is at -1.112 V, see Figure S5. The difference to -0.964 V of **8** could be interpreted by a stabilizing effect of the negative charge by the second neutral PBI in the mixed valence **8**⁻). The third reduction occurs with $E_{1/2} = -1.426$ V at much more negative potential (PBI^{•••}PBI → PBI^{2•••}PBI), but is immediately followed by a chemical reaction ($K = k_f/k_b = 19.9$ with $k_f > 10^6$ s⁻¹) that we relate to the separation of the two PBI π -faces and concomitant opening of the cyclophane cavity (PBI^{2•••}PBI \rightleftharpoons PBI^{2••••}PBI, see below) which is caused by the increased electrostatic repulsion in the trianion. The subsequent fourth reduction which leads to the tetraanion, occurs at a formally more positive potential ($E_{1/2} = -1.124$ V) than the third reduction because of less Coulomb repulsion in the widened cyclophane. These last two reduction processes can be seen in the CV by a scan rate dependent (see Figure S4) third wave around -1.5 V. Consequently, back oxidation is at even more positive potentials than the second reduction and covers the transfer of three electrons. This is seen as a strong anodic signal at -1.1 V. The following anodic peak at -0.95 V refers to the fourth oxidation step to yield the neutral cyclophane **8**. The whole redox cycle is chemically fully reversible on a long term scale (30 min) as has been proved by thin-layer measurements (see inset in Figure 3 and Figure S6 in Supporting Information).

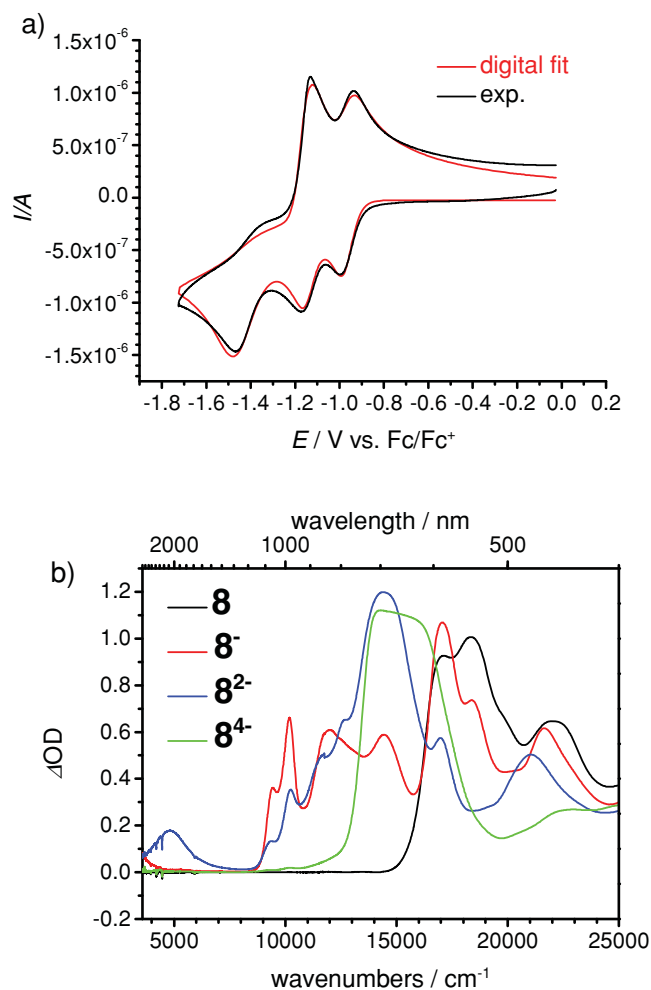


Figure 2. a) Cyclic voltammogram of **8** in DCM/ 0.2 M TBAH at $\nu = 250$ mV s⁻¹ vs Fc/Fc⁺ and digital fit by DigiSim. b) Spectroelectrochemistry of **8**; the spectra shown were obtained by deconvolution with SpecFit and refer to the hypothetically isolated species.

While the interpretation of the CVs seems plausible, proof for this postulated mechanism is gained by UV/Vis/NIR spectroelectrochemistry of the reduced species in a thin-layer (ca. 100 μ m) at a reflective platinum working electrode.^[25] In this experiment, a series of UV/Vis/NIR spectra were recorded in reflection at a polished platinum working electrode while the potential was varied stepwise in 20 mV steps. The spectra of the hypothetically isolated reduced species were then evaluated by deconvolution with SpecFit (see Figure 2b and also Figure S7 in Supporting Information). As expected from the model in Figure 3, the spectrum of the monoanion **8**⁻ (Figure 2b, red) shows spectral features of both the neutral PBI (two bands at ca. 17000–19000 cm⁻¹) and of the singly reduced PBI (two sharp peaks at ca. 10000 cm⁻¹ and a very prominent signal at 14000 cm⁻¹). In addition, there is the onset of a weak band visible below 4000 cm⁻¹ which has intervalence charge transfer (IV-CT) character,^[26] and is due to an optically induced electron transfer from PBI⁻ to the neutral PBI in the mixed valence cyclophane **8**. This feature is in agreement with the one recently

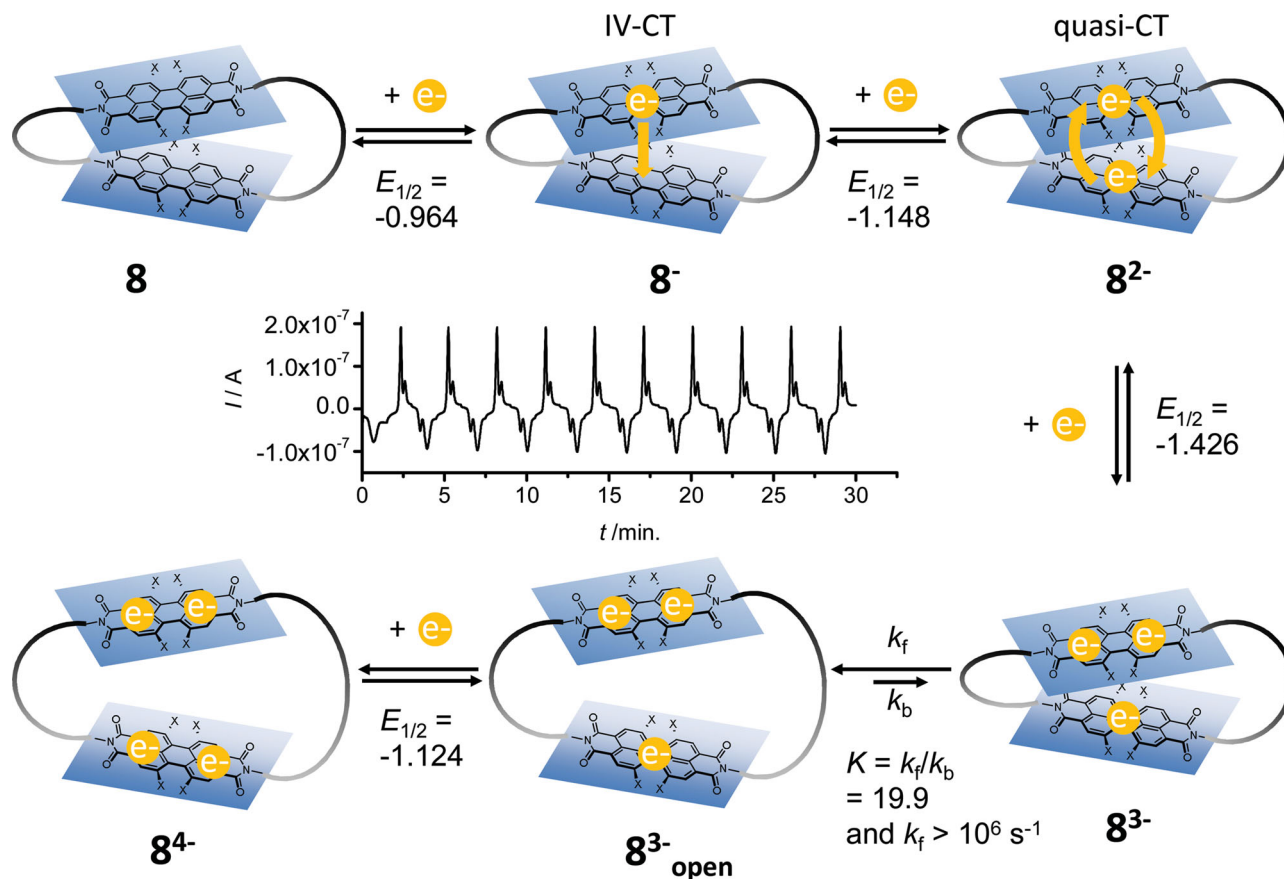


Figure 3. Reduction processes and reversible contraction/expansion of cyclophane **8**. The redox potentials and equilibrium constant were obtained by digital fit to the cyclic voltammograms at different scan rate. The inset shows 10 thin-layer voltammograms vs time at $\nu = 10 \text{ mV s}^{-1}$. Switching potentials are $-0.6/-1.5 \text{ V}$.

observed in a PBI dimer linked by a single σ -bond at the bay positions.^[27] In the dianion 8^{2-} the spectral feature of the PBI⁻ at 14000 cm^{-1} increases in intensity, whilst that of neutral PBI at 17000 cm^{-1} decreases (Figure 2b, blue). Furthermore, a moderately strong absorption at 5000 cm^{-1} appears, which is also seen in the σ -bonded PBI dimer, which is caused by a “quasi-CT” process in which an electron of this biradical dianion is excited from the one PBI to the other and vice versa.^[27] The trianion is not visible in the spectroelectrochemistry because its intermediate concentration vanishes due to the very fast follow-up process (ring expansion) and reduction to the tetraanion at even higher potential. The latter shows spectral features (broad and intense band at ca. 15000 cm^{-1} , Figure 2b, green) very similar to the dianion of the reference compound **7** (Figure S7) and other tetraphenoxo PBIs.^[28]

The UV/Vis/NIR spectra of reduced species **8** impressively support the above outlined redox-dependent ring expansion/contraction mechanism. Most importantly, they prove that pronounced electronic interactions between the two PBIs are manifested by IV-CT and quasi-CT processes in the mono- and dianion which requires spatial proximity, whereas no interactions are evident in the fully reduced tetraanion due to the larger PBI separation (almost identical spectra to that of 7^{2-}).

The changes in Coulomb repulsion between the closed and the expanded cyclophane macrocycle involves the conversion of about 30 kJ/mol of electrical into mechanical energy and suggests a bistability^[29,30] for species 8^{3-} . Our current research is devoted towards the elucidation of this bistability, the evaluation of the distance changes upon expansion/contraction (“molecular actuation”)^[9,31] and the capturing of small molecules/ions in the expanded macrocycle.

Supporting Information

Supporting Information is available from the Wiley Online Library or from the author.

Acknowledgements

We gratefully acknowledge financial support for this project by the DFG Research Unit “Light-Induced Dynamics in Molecular Aggregates” (FOR 1809).

Received: March 27, 2012
Published online:

- [1] a) V. Balzani, A. Credi, F. M. Raymo, J. F. Stoddart, *Angew. Chem. Int. Ed.* **2000**, *39*, 3348–3391; b) K. Kinbara, T. Aida, *Chem. Rev.* **2005**, *105*, 1377–1400; c) V. Balzani, A. Credi, M. Venturi, *Molecular Devices and Machines*. Wiley-VCH: Weinheim, 2nd edn, **2008**; d) S. Silvi, M. Venturi, A. Credi, *Chem. Commun.* **2011**, *47*, 2483–2489; e) A. Coskun, M. Banaszak, R. D. Astumian, J. F. Stoddart, B. A. Grzybowski, *Chem. Soc. Rev.* **2012**, *41*, 19–30.
- [2] a) W. R. Browne, B. L. Feringa, *Nat. Nanotechnol.* **2006**, *1*, 25–35; b) E. R. Kay, D. A. Leigh, F. Zerbetto, *Angew. Chem. Int. Ed.* **2007**, *46*, 72–191.
- [3] a) C. O. Dietrich-Buchecker, J. P. Sauvage, *Chem. Rev.* **1987**, *87*, 795–810; b) D. B. Amabilino, J. F. Stoddart, *Chem. Rev.* **1995**, *95*, 2725–2828.
- [4] a) H. Tian, Q.-C. Wang, *Chem. Soc. Rev.* **2006**, *35*, 361–374; b) S. Silvi, M. Venturi, A. Credi, *J. Mater. Chem.* **2009**, *19*, 2279–2294.
- [5] a) R. A. Bissell, E. Cordova, A. E. Kaifer, J. F. Stoddart, *Nature* **1994**, *369*, 133–137; b) C. P. Collier, G. Matternsteig, E. W. Wong, Y. Luo, K. Beverly, J. Sampaio, F. M. Raymo, J. F. Stoddart, J. R. Heath, *Science* **2000**, *289*, 1172–1175; c) S. A. Vignon, T. Jarroson, T. Iijima, H.-R. Tseng, J. K. M. Sanders, J. F. Stoddart, *J. Am. Chem. Soc.* **2004**, *126*, 9884–9885.
- [6] a) A. M. Brouwer, C. Frochot, F. G. Gatti, D. A. Leigh, L. Mottier, F. Paolucci, S. Roffia, G. W. H. Wurpel, *Science* **2001**, *291*, 2124–2128; b) G. Fioravanti, N. Haraszkiwicz, E. R. Kay, S. M. Mendoza, C. Bruno, M. Marcaccio, P. G. Wiering, F. Paolucci, P. Rudolf, A. M. Brouwer, D. A. Leigh, *J. Am. Chem. Soc.* **2008**, *130*, 2593–2601.
- [7] a) R. A. van Delden, M. K. J. ter Wiel, M. M. Pollard, J. Vicario, N. Koumura, B. L. Feringa, *Nature* **2005**, *437*, 1337–1340; b) R. Eelkema, M. M. Pollard, J. Vicario, N. Katsonis, B. S. Ramon, C. W. M. Bastiaansen, D. J. Broer, B. L. Feringa, *Nature* **2006**, *440*, 163–163.
- [8] a) F. Würthner, J. Rebek Jr., *Angew. Chem. Int. Ed. Engl.* **1995**, *34*, 446–448; b) T. Muraoka, K. Kinbara, Y. Kobayashi, T. Aida, *J. Am. Chem. Soc.* **2003**, *125*, 5612–5613; c) D. Blegler, T. Liebig, R. Thiermann, M. Maskos, J. P. Rabe, S. Hecht, *Angew. Chem. Int. Ed.* **2011**, *50*, 12559–12563.
- [9] a) C. Song, T. M. Swager, *Org. Lett.* **2008**, *10*, 3575–3578; b) H. Yu, T. M. Swager, *IEEE J. Oceanic Eng.* **2004**, *29*, 692–695.
- [10] Z. Chen, A. Lohr, C. R. Saha-Möller, F. Würthner, *Chem. Soc. Rev.* **2009**, *38*, 564–584.
- [11] a) J. Salbeck, H. Kunkely, H. Langhals, R. W. Saalfrank, J. Daub, *Chimia* **1989**, *43*, 6–9; b) S. K. Lee, Y. B. Zu, A. Herrmann, Y. Geerts, K. Müllen, A. J. Bard, *J. Am. Chem. Soc.* **1999**, *121*, 3513–3520.
- [12] For reviews on self-assemblies of PBI dyes, see: a) F. Würthner, *Chem. Commun.* **2004**, 1564–1579; b) M. R. Wasielewski, *J. Org. Chem.* **2006**, *71*, 5051–5066; c) J. A. A. W. Elemans, R. van Hameren, R. J. M. Nolte, A. E. Rowan, *Adv. Mater.* **2006**, *18*, 1251–1266; d) C. Huang, S. Barlow, S. R. Marder, *J. Org. Chem.* **2011**, *76*, 2386–2407; 12 For some examples on covalently tethered or macrocyclic systems bearing two PBI dyes in highly defined conformations, see: e) J. M. Giaimo, A. V. Gusev, M. R. Wasielewski, *J. Am. Chem. Soc.* **2002**, *124*, 8530–8531; f) D. Veldman, S. M. A. Chopin, S. C. J. Meskers, M. M. Groeneveld, R. M. Williams, R. A. J. Janssen, *J. Phys. Chem. A* **2008**, *112*, 5846–5857; g) C. Hippius, I. H. M. van Stokkum, E. Zangrando, R. M. Williams, M. Wykes, D. Beljonne, F. Würthner, *J. Phys. Chem. C* **2008**, *112*, 14626–14638; h) J. Feng, Y. Zhang, C. Zhao, R. Li, W. Xu, X. Li, J. Jiang, *Chem. Eur. J.* **2008**, *14*, 7000–7010.
- [13] Structural relaxation processes in the photoexcited state have been reported, e.g., see: R. F. Fink, J. Seibt, V. Engel, M. Renz, M. Kaupp, S. Lochbrunner, H.-M. Zhao, J. Pfister, F. Würthner, B. Engels, *J. Am. Chem. Soc.* **2008**, *130*, 12858–12859.
- [14] B. Speiser, in *Modern Cyclophane Chemistry* (Eds: R. Gleiter, H. Hopf), Wiley-VCH, Weinheim, Germany **2004**, p. 359.
- [15] a) S. Amthor, C. Lambert, B. Graser, D. Leusser, C. Selinka, D. Stalke, *Org. Biomol. Chem.* **2004**, *2*, 2897–2901; b) S. Amthor, C. Lambert, *J. Phys. Chem. A* **2006**, *110*, 1177–1189; c) S. Amthor, C. Lambert, *J. Phys. Chem. A* **2006**, *110*, 3495–3504.
- [16] a) S. Höger, *J. Polym. Sci. A* **1999**, *37*, 2685–2698; b) S. Höger, *Angew. Chem. Int. Ed.* **2005**, *44*, 3806–3808; c) M. Iyoda, J. Yamakawa, M. J. Rahman, *Angew. Chem. Int. Ed.* **2011**, *50*, 10522–10553.
- [17] H. Enozawa, M. Hasegawa, D. Takamatsu, K. Fukui, M. Iyoda, *Org. Lett.* **2006**, *8*, 1917–1920.
- [18] S. Anderson, H. L. Anderson, J. K. M. Sanders, *Acc. Chem. Res.* **1993**, *26*, 469–475.
- [19] Despite their bulky bay substituents 1,6,7,12-tetraphenoxy-substituted PBIs are prone to aggregation into π - π -stacked dimers, see: Z. Chen, U. Baumeister, C. Tschierske, F. Würthner, *Chem. Eur. J.* **2007**, *13*, 450–465.
- [20] Q. Zhou, P. J. Carroll, T. M. Swager, *J. Org. Chem.* **1994**, *59*, 1294–1301.
- [21] J. Seibt, P. Marquetand, V. Engel, Z. Chen, V. Dehm, F. Würthner, *Chem. Phys.* **2006**, *328*, 354–362.
- [22] M. Kasha, H. R. Rawls, M. A. El-Bayoumi, *Pure Appl. Chem.* **1965**, *11*, 371–392.
- [23] M. Hesse, H. Meier, B. Zeeh, *Spectroscopic Methods in Organic Chemistry*. Thieme: Stuttgart, **1997**.
- [24] A.W. Bott, S.W. Feldberg, M. Rudolph, *Current Separations* **1996**, *15*, 67–71.
- [25] J. Salbeck, *J. Electroanal. Chem.* **1992**, *340*, 169–195.
- [26] A. Heckmann, C. Lambert, *Angew. Chem. Int. Ed.* **2012**, *51*, 326–392.
- [27] W. Jiang, C. Xiao, L. Hao, Z. Wang, H. Ceymann, C. Lambert, S. Di Motta, F. Negri, *Chem. Eur. J.* **2012**, *18*, 6764.
- [28] F. Würthner, A. Sautter, D. Schmid, P. J. A. Weber, *Chem. Eur. J.* **2001**, *7*, 894–902.
- [29] a) G. Tsekouras, N. Minder, E. Figgemeier, O. Johansson, R. Lomoth, *J. Mater. Chem.* **2008**, *18*, 5824–5829; b) A. Tomita, M. Sano, *Inorg. Chem.* **2000**, *39*, 200–205; c) V. Amendola, C. Mangano, P. Pallavicini, M. Zema, *Inorg. Chem.* **2003**, *42*, 6056–6062; d) T. Hamaguchi, K. Ujimoto, I. Ando, *Inorg. Chem.* **2007**, *46*, 10455–10457.
- [30] This value is an estimation based on $\Delta G^0 = -n \times F \times \Delta E$ that only considers the difference in the redox potential for the third electron ($n = 1$) in the oxidative and reductive step $\Delta E \approx 1.4 - 1.1 \text{ V} = 0.3 \text{ V}$ with the Faraday constant $F = 96485 \text{ C/mol}$.
- [31] K. Miwa, Y. Furusho, E. Yashima, *Nature Chem.* **2010**, *2*, 444–449.